Recovering Young's moduli in heterogeneous stenosed carotid arteries: a numerical plane strain study

Alexandre Franquet, Stéphane Avril, Rodolphe Le Riche, Pierre Badel

RECOVERING YOUNG MODULI IN HETEROGENEOUS STENOSED CAROTID ARTERIES: A NUMERICAL PLANE STRAIN STUDY.

A. Franquet[1], S. Avril[2], R. Le Riche[3] and P. Badel[4]

1. ABSTRACT

Assessing the vulnerability of atherosclerotic plaques requires an accurate knowledge of the mechanical properties of the plaque constituents. It is possible to measure displacements *in vivo* inside a plaque using ultrasounds or magnetic resonance imaging. The main issue is to solve the inverse problem that consists in estimating the elastic properties inside the plaque from measured displacements.
This study focuses on the identifiability of elastic parameters. An idealised plane strain Finite Element (FE) model is used.

2. INTRODUCTION

Ripping-off of atherosclerotic plaques in carotid arteries is a major cause of mortality in OECD countries. ECST[5] study has shown that patients with a stenosis larger than 70% benefit from a surgical intervention. Due to remodelling, this geometrical criterion alone may be insufficient for asymptomatic patients.
It has been shown in the literature that the vulnerability of an atherosclerotic plaque can also be assessed with a maximum stress criterion [1]. The calculation of this criterion requires an accurate knowledge of the mechanical properties of the plaque constituents.
While the medical objective is obvious, the main issue remains the estimation of the mechanical properties of the plaque constituents *in vivo*. It involves the definition of an inverse problem consisting in finding the mechanical properties of a numerical model that fits experimental displacements.
It is possible to measure displacements between diastolic and systolic pressure in diseased arteries and using ultrasounds [2] or MRI [3]. The heterogeneities contours can also be obtained by image processing [4].
Most of the time the reconstruction of mechanical properties in arteries utilises FE model updating [5,6]. Authors have focused on optimisation algorithms [7,8] and on methods for improving the mechanical properties mapping [5]. Le Floc'h explained in [6] how to choose the FE model parameters (number of elements, element type...). Two types of uncertainties can affect the identification: numerical approximations (type I) or experimental errors (type II).
The elastic parameters identifiability is studied in this article. In particular, the effects of the FE mesh and of the *a priori* parameters values are studied (type I), as well as the

[1]PhD student, Centre for Health and Engineering PECM CNRS UMR 5146 and IFRESIS INSERM IFR 143, Ecole des Mines de Saint-Etienne, 158 cours Fauriel 42023 Saint-Etienne cedex 2 FRANCE
[2] Senior lecturer, Center for Health Engineering PECM CNRS UMR 5146 / IFRESIS INSERM IFR 143, Ecole des Mines de Saint-Etienne, 158 cours Fauriel 42023 Saint-Etienne cedex 2 FRANCE
[3]CNRS permanent research associate, Ecole des Mines de Saint-Etienne, 158 cours Fauriel 42023 Saint-Etienne cedex 2 FRANCE
[4] Lecturer, Center for Health Engineering PECM CNRS UMR 5146 / IFRESIS INSERM IFR 143, Ecole des Mines de Saint-Etienne, 158 cours Fauriel 42023 Saint-Etienne cedex 2 FRANCE
[5]European Carotid Surgery Trial

effects of the interpolation grid size and of white noise corrupting experimental data (type II).

3. METHODS

3.1 FE model

An idealised atherosclerotic carotid artery in 2D has been modelled in a manner inspired by [1] (cf. Fig.1). Dimensions correspond to a 66% stenosis. The mechanical behaviour is supposed to be linear elastic, under the hypothesis of plane strain. One node has been blocked in the $\vec{x}$ and $\vec{y}$ directions, and one node has been blocked in the $\vec{y}$ direction to remove rigid body motion. A pressure of 5 kPa is applied uniformly on the artery wall, simulating the differential pressure of a patient between diastole and systole. Quasi-static conditions are assumed as the heart beats have approximately a frequency of 1 Hz. Three different materials are defined (cf. Fig.1):

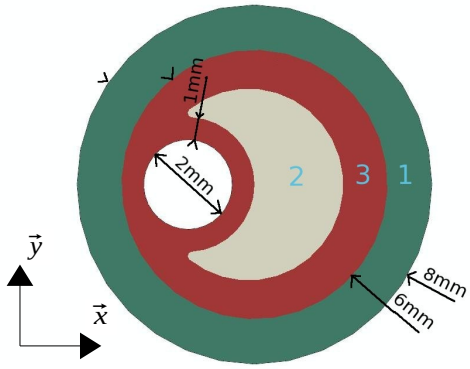

Fig. 1: Dimensions and materials of the model.

1) Healthy tissue.
2) A lipidic core composed essentially of fat.
3) Diseased tissue including the fibrous cap and a part of the infected *media*, more rigid than the healthy tissue.

3.2 Synthetic data

The behaviour of arteries is supposed to be quasi-incompressible (fluid saturated materials). The elastic properties of the three materials are set to the following values:

1) Healthy tissue: $E_{Healthy\ tissue} = E_{HT} = 600\,\text{kPa}$ and $\nu_{Healthy\ tissue} = \nu_{HT} = 0.49$.
2) Lipidic core: $E_{Lipidic\ core} = E_{LC} = 10\,\text{kPa}$ and $\nu_{Lipidic\ core} = \nu_{LC} = 0.49$.
3) Diseased tissue: $E_{Diseased\ tissue} = E_{DT} = 800\,\text{kPa}$ and $\nu_{Diseased tissue} = \nu_{DT} = 0.49$.

The synthetic data is the result of the computation of a FE model with about 130 000 CPE8H elements[6]. The solution is then interpolated on a regular N by N grid with a step S, which simulates an MRI output with the voxel size S.

3.3 Inverse approach

An inverse approach consists in finding the parameters of a system, knowing its response. The principle is to minimise a distance J_2 (cf. Eq.1) with an optimisation algorithm.

$$J_2(\vec{\theta}) = \sum_{i=0}^{N} (U_i(\vec{\theta}) - Usynthetic_i)^2 \qquad (1)$$

with here:

- N : Number of interpolating nodes (grid nodes).

[6]The CPE8H element is the element recommended by Abaqus®(software used) in quasi-incompressible cases.

- $\vec{\theta}$: Vector of parameters, Young moduli and Poisson ratios depending on the test cases (see later).
- $U_i(\vec{\theta})$: Displacement from a FE simulation interpolated at the grid node i .
- $Usynthetic_i$: Synthetic displacement at the grid node i .

A Levenberg-Marquardt algorithm with bounds handling is used to recover the elastic properties. Two termination criteria are set up:

- $\|\Delta\vec{\theta}\| \leq 10^{-25}$: Step $\|\Delta\vec{\theta}\|$ too small. No more improvement is expected.
- $J_2(\vec{\theta}_j) \leq 10^{-7}$: The accuracy on J_2 is reached.

The Levenberg-Marquardt algorithm requires at each iteration the matrix of gradients $\overline{\nabla_{\vec{\theta}}}(\vec{U}(\vec{\theta}))$ which is calculated by backward finite differences.

3.4 Definition of numerical experiments

Four different tests are proposed which focus on the identification of mechanical properties quality. The values identified by the optimisation algorithm are compared to the synthetic ones. The following configuration is considered as default:

Mesh types	CPE6 5000 and CPE8H 5000
Grid step size for the synthetic data	0.125 mm
Number and type of unknown parameters	$\{E_{Healthy\,tissue}, E_{Lipidic\,core}, E_{Diseased\,tissue}\}$
Set of Poisson ratios	$\{\nu_{Healthy\,tissue}, \nu_{Lipidic\,core}, \nu_{Diseased\,tissue}\} = \{0.49, 0.49, 0.49\}$
Initial vector of parameters	$\vec{\theta} = \{E_{Healthy\,tissue} = 1000\,\text{kPa}, E_{Lipidic\,core} = 100\,\text{kPa}, E_{Diseased\,tissue} = 1200\,\text{kPa}\}$

Tab. 1:Default values

1) Effect of the FE mesh:

Two different elements are tested: the CPE6 element (Continuum Plane Strain 6 nodes element, triangle, used in [6]) and the CPE8H element (Continuum Plane Strain 8 nodes element with hybrid formulation, quadrangle, recommended by Abaqus®). Four numbers of elements are tested: 1000, 5000, 15000 and 40000.

2) Effect of the *a priori* Poisson ratios:

Poisson ratios are voluntarily set to wrong values during the identification procedure:

$$\{\nu_{Healthy\,tissue}, \nu_{Lipidic\,core}, \nu_{Diseased\,tissue}\} = \{\{0.45, 0.45, 0.45\}, \{0.48, 0.48, 0.48\}, \{0.499, 0.499, 0.499\}\} \quad (2)$$

3) Effect of the grid step size:

The grid step size is directly linked to the MRI spacial resolution. The synthetic data are interpolated on a regular grid with the step size S taken as:

$$Step_{size} = \{1\,\text{mm}, 0.5\,\text{mm}, 0.25\,\text{mm}, 0.125\,\text{mm}\} \quad (3)$$

4) Effect of white Gaussian noise:

Experimental data always contain noise. The effect of white Gaussian noise on synthetic data is studied. The synthetic displacements are defined as:

$$\begin{aligned} \vec{U}^{x}_{synthetic} &= \vec{U}^{x}_{synthetic} + \sigma \times \vec{R}_1 \\ \vec{U}^{y}_{synthetic} &= \vec{U}^{y}_{synthetic} + \sigma \times \vec{R}_2 \end{aligned} \quad (4)$$

with:

- $\sigma = 3\% \times \text{mean}(\|\vec{U}_{synthetic}\|)$: standard deviation.
- $\vec{R}_1$ and $\vec{R}_2$: random vectors following a standard normal law $\mathcal{N}(0,1)$.

In order to estimate means and standard deviations of each identified value the identification is repeated twenty times.

4. RESULTS

4.1 Effect of the FE mesh

Mesh type		E_{HA} (kPa)	$\%E_{HA}$	E_{LC}	E_{LC}	E_{DT}	E_{DT}	Time (s)		Termination Criterion
Reference		*600*		*10.00*		*800*		1 FE_{sim}	Total	
CPE6	1000	607	1.24%	9.77	-2.33%	798	-0.29%	0.38	590	$\|\Delta\vec{\theta}\| \le 10^{-25}$
	5000	603	0.55%	9.94	-0.56%	799	-0.07%	1.19	1077	$\|\Delta\vec{\theta}\| \le 10^{-25}$
	15000	604	0.68%	10.02	0.24%	799	-0.06%	3.99	858	$J_2(\vec{\theta}_j) \le 10^{-7}$
	40000	603	0.53%	10.04	0.44%	800	-0.05%	10.66	2063	$J_2(\vec{\theta}_j) \le 10^{-7}$
CPE8H	1000	602	0.43%	9.97	-0.33%	800	-0.06%	0.84	803	$\|\Delta\vec{\theta}\| \le 10^{-25}$
	5000	603	0.64%	10.04	0.39%	800	-0.06%	3.83	573	$J_2(\vec{\theta}_j) \le 10^{-7}$
	15000	604	0.54%	10.04	0.43%	800	-0.05%	12.39	1449	$J_2(\vec{\theta}_j) \le 10^{-7}$
	40000	603	0.47%	10.05	0.51%	800	-0.04%	44.63	4440	$J_2(\vec{\theta}_j) \le 10^{-7}$

Tab. 2: Identifications with different meshes.

The identification quality for the CPE6 element reveals a difference with real values always lower than 2.4%. The error on final Young moduli of CPE8H optimisations are always lower than 0.7% whatever the number of elements is. Both termination criteria appear, suggesting that both are useful. The J_2 index has not reached the limit in three cases, but the identification quality is lower than 2.4%.

This test leads to the selection of two meshes for the next numerical experiments:

- CPE6 5000: Although the accuracy on J_2 has not been reached, the algorithm already finds a vector $\vec{\theta}_{final}$ after 346 seconds:
  $\vec{\theta}_{final} = \{E_{Healthy\,tissue} = 606\,\text{kPa}, E_{Lipidic\,core} = 9.99\,\text{kPa}, E_{Diseased\,tissue} = 799.18\,\text{kPa}\}$
- CPE8H: The identification quality is good (<1% on all Young modulus), and the identification total time (573 seconds) is the lowest among identifications which converged.

4.2 Effect of the *a priori* Poisson ratios

Mesh	Sets of Poisson ratios			Identified Young moduli						Total time (s)
	ν_{HA}	ν_{LC}	ν_{DT}	E_{HA} (kPa)	$\%E_{HA}$	E_{LC}	$\%E_{LC}$	E_{DT}	$\%E_{DT}$	
Ref.	0.49	0.49	0.49	*600*		*10.00*		*800*		
CPE6 5000	0.45	0.45	0.45	650	8.26%	17.90	78.99%	804	0.45%	1017
	0.48	0.48	0.48	633	5.47%	13.65	36.48%	793	-0.87%	1002
	0.49	0.49	0.49	603	0.55%	9.94	-0.56%	799	-0.07%	1038
	0.499	0.499	0.499	394	-34.36%	1.23	-87.74%	844	5.53%	1187
	0.45	0.45	0.45	648	8.03%	17.92	79.22%	804	0.47%	1579

CPE8H 5000	0.48	0.48	0.48	631	5.21%	13.69	36.88%	793	-0.84%	1620
	0.49	0.49	0.49	604	0.64%	10.04	0.39%	800	-0.06%	557
	0.499	0.499	0.499	387	-35.43%	1.22	-87.82%	845	5.68%	2063

Tab. 3: Identifications with different sets of Poisson ratios.

An underestimation of 8% on the Poisson ratios leads to errors of 8% on the healthy artery Young modulus, and 80% on the lipidic core Young modulus for both meshes, whereas an underestimation of 2% on the Poisson ratios leads to errors of respectively 5% and 37%. The Young modulus of the diseased tissue is only affected in the case of an overestimation of the Poisson ratios.

4.3 Effect of the grid step size

Mesh	Step size (mm)	E_{HA} (kPa)	$\%E_{HA}$	E_{LC}	$\%E_{LC}$	E_{DT}	$\%E_{DT}$	Total time (s)	Termination criterion
Ref.		*600*		*10.00*		*800*			
CPE6 5000	1	655	9.12%	10.76	7.62%	795	-0.64%	462	$J_2(\vec{\theta}_j) \leq 10^{-7}$
	0.5	607	1.16%	10.01	0.11%	799	-0.12%	443	$J_2(\vec{\theta}_j) \leq 10^{-7}$
	0.25	606	1.04%	10.00	-0.01%	799	-0.11%	392	$J_2(\vec{\theta}_j) \leq 10^{-7}$
	0.125	603	0.55%	9.94	-0.56%	799	-0.07%	1038	$\|\Delta \vec{\theta}\| \leq 10^{-25}$
CPE8H 5000	1	654	8.99%	10.83	8.26%	795	-0.63%	802	$J_2(\vec{\theta}_j) \leq 10^{-7}$
	0.5	605	0.87%	10.06	0.65%	799	-0.07%	753	$J_2(\vec{\theta}_j) \leq 10^{-7}$
	0.25	604	0.74%	10.05	0.50%	799	-0.07%	653	$J_2(\vec{\theta}_j) \leq 10^{-7}$
	0.125	604	0.64%	10.04	0.39%	800	-0.06%	557	$J_2(\vec{\theta}_j) \leq 10^{-7}$

Tab. 4: Identifications with different grid step sizes.

The results between the two types of elements are very similar in terms of accuracy. With the larger step size (1mm), the error on the healthy artery Young modulus is 9% and the error on the lipidic core is 8%. The identification time decreases shortly when the step size decreases. With a given step size, for instance 1 mm, the CPE6 identification is twice faster the CPE8H one.

4.4 Effect of white Gaussian noise

Mesh		E_{HA} (kPa)	$\%E_{HA}$	E_{LC}	$\%E_{LC}$	E_{DT}	$\%E_{DT}$	Total time (s)
Ref.		*600*		*10.00*		*800*		
CPE6 5000	Mean	603	0.52%	9.93	-0.65%	799	-0.08%	1114
	Standard deviation	1.28	0.21%	0.03	0.26%	0.25	0.03%	48
CPE8H 5000	Mean	601	0.17%	9.98	-0.20%	800	-0.03%	1768
	Standard deviation	1.28	0.21%	0.03	0.26%	0.25	0.03%	61

Tab. 5: Identifications with 3% of white Gaussian noise in the synthetic data.

All the identifications made in this section terminated because of $\|\Delta \vec{\theta}\| \leq 10^{-25}$. The noise added to the synthetic data affects both element types in the same way in terms of Young moduli standard deviations (respectively 0.21%, 0.30%, 0.03%).

5. DISCUSSION AND CONLUSION

Comments on two aspects can be distinguished:

1. Computation time and termination criteria

Computation time can be saved with a good choice of FE model (FE model with 5000 CPE6 elements shows generally an identification quality <1%). A less stringent choice of threshold for the second termination criterion ($\|\Delta\vec{\theta}\| \leq 10^{-8}$ for instance) could significantly reduce the identification time when this criterion is predominant. We also raises questions about the interpretation of the absolute value of J_2 which can be low but still leading to erroneous Young moduli and *vice versa*.

The grid step size has no obvious effect on the accuracy of the identified Young moduli from the step size 0.5 mm.

2. Poisson ratio estimation

The estimation of the Poisson ratios has the strongest influence on the accuracy of the identified values. Note that the algorithm tends to rigidify the healthy artery and the lipidic core to compensate an underestimation of Poisson ratios of the lipidic core and the healthy artery and *vice versa*.

Further investigations are currently led to simulate real experimental noise and to work with more realistic experimental data.

6. REFERENCES

1. Li Z. Y., Tang T., U-King-Im J., Graves M. J., Sutcliffe M. and Gillard J. H., Assessment of carotid plaque vulnerability using structural and geometrical determinants., Circ J, 2008, Vol. 72, 1092-1099.
2. Ophir J., Kallel F., Varghese T., Konofagou E., Alam S. K., Krouskop T., Garra B. and Righetti R., Elastography, C R Acad Sci Paris, 2001, Serie IV, 1193-1212.
3. Avril S., Huntley J., Pierron F. and Steele D., 3D Heterogeneous Stiffness Reconstruction Using MRI and the Virtual Fields Method, Exp Mech, 2008,Vol. 48, 479–494
4. Hermus L., van Dam G. M. and Zeebregts C. J., Advanced Carotid Plaque Imaging, Eur J Vasc Endovasc Surg, 2010, Vol. 39, 125-133.
5. Baldewsing R. A., Danilouchkine M. G., Mastik F., Shaar J. A., Serruys P. W. and van der Steen A. F. W., An Inverse Method for Imaging the Local Elasticity of Atherosclerotic Coronary Plaques, IEEE T Inf Technol B, 2008, Vol. 12, 277-289.
6. Le Floc'h S., Modulographie vasculaire : Application à l'identification in-vivo du module de Young local des plaques d'athérosclérose, PhD thesis University of Grenoble (France), 2009.
7. Khalil A. S., Bouma B. E. and Kaazempour M. M. R., A combined FEM/Genetic Algorithm for Vascular Soft Tissue Elasticity Estimation, Cardiovasc Eng, 2006, Vol. 6, 95-104.
8. Fehrenbach J., Masmoudi M., Souchon R. and Trompette P., Detection of small Inclusions by Elastography, Inverse Probl, 2006, Vol. 22, 1055-1069.